PCCP

RSC Publishing

PAPER

View Article Online
View Journal | View Issue

Cite this: *Phys. Chem. Chem. Phys.*, 2013, **15**, 4651

The influence of electron injection and charge recombination kinetics on the performance of porphyrin-sensitized solar cells: effects of the 4-*tert*-butylpyridine additive†

Yu-Cheng Chang,[a] Hui-Ping Wu,[a] Nagannagari Masi Reddy,[b] Hsuan-Wei Lee,[b] Hsueh-Pei Lu,[a] Chen-Yu Yeh*[b] and Eric Wei-Guang Diau*[a]

Received 17th December 2012,
Accepted 4th February 2013

DOI: 10.1039/c3cp44555k

www.rsc.org/pccp

The effects of the 4-*tert*-butylpyridine (TBP) additive in the electrolyte on photovoltaic performance of two push–pull porphyrin sensitizers (YD12 and YD12CN) were examined. Addition of TBP significantly increased the open-circuit voltage (V_{OC}) for YD12 (from 550 to 729 mV) but it was to a lesser extent for YD12CN (from 544 to 636 mV); adding TBP also had the effect of reducing the short-circuit current density (J_{SC}) slightly for YD12 (from 17.65 to 17.19 mA cm^{-2}) but it led to a significant reduction for YD12CN (from 16.45 to 9.78 mA cm^{-2}). The resulting power conversion efficiencies of the YD12 devices increase from 6.2% to 8.5% whereas those of the YD12CN devices decrease from 5.8% to 4.5%. Based on measurements of temporally resolved photoelectric transients of the devices and femtosecond fluorescence decays of thin-film samples, the poor performance of the YD12CN device in the presence of TBP can be understood as being due to the enhanced charge recombination, decreased electron injection, and a lesser extent of inhibition of the intermolecular energy transfer.

1. Introduction

Dye-sensitized solar cells (DSSCs) are promising next-generation photovoltaic devices because of their great advantages such as light weight, low cost and easy processing, with colourful and transparent features.[1] Photosensitizers such as ruthenium complexes,[1,2] zinc porphyrins[3] and metal-free organic dyes[4] have been developed to serve as efficient light harvesters for DSSCs. As a result, the devices made of ruthenium complexes[5] and porphyrin sensitizers[6] have attained remarkable power conversion efficiencies, η = 11.0–11.5%, under one-sun illumination. Recently, it has been reported that co-sensitization of a push–pull zinc porphyrin (YD2-oC8) with an organic dye (Y123) using a cobalt-based redox electrolyte boosted the cell performance to η = 12.3%,[7] stimulating the investigation of the development of new porphyrin sensitizers to further enhance the device performance of DSSCs.

The molecular structure of a highly efficient push–pull porphyrin sensitizer features an electron donor group attached at the *meso*-position of the porphyrin core opposite to the *meso*-substituted linker with a carboxylic acid serving as an anchoring group for dye sensitization of the surface of TiO_2. For the YD2-series dyes,[6–8] the electron donor is a diarylamino derivative and the π-conjugated linker involves a phenylethynyl (PE) moiety. Previously we found that modification of the PE linker by substituting the phenyl group with a naphthalene unit (YD12) enhances the device performance due to its superior light-harvesting ability.[9] In the present study, we design a porphyrin sensitizer (YD12CN) based on the structure of YD12 with the same donor group but using the cyanoacrylic acid as an anchoring group, which is widely employed in the molecular design of an organic dye.[4] The molecular structures of YD12 and YD12CN are indicated in Chart 1. The effects of the 4-*tert*-butylpyridine (TBP) additive on photovoltaic performance were examined based on the measurements of charge extraction, transient photoelectric decays, and femtosecond fluorescence decays.

[a] *Department of Applied Chemistry and Institute of Molecular Science, National Chiao Tung University, Hsinchu 30010, Taiwan. E-mail: diau@mail.nctu.edu.tw; Fax: +886-3-5723764; Tel: +886-3-5131524*
[b] *Department of Chemistry and Center of Nanoscience & Nanotechnology, National Chung Hsing University, Taichung 402, Taiwan. E-mail: cyyeh@dragon.nchu.edu.tw; Fax: +886-4-22862547; Tel: +886-4-22852264*

† Electronic supplementary information (ESI) available: Experimental details of syntheses, device fabrication, photovoltaic and time-resolved investigations, together with supplementary figures, Fig. S1–S12, and supplementary tables, Tables S1–S7. See DOI: 10.1039/c3cp44555k

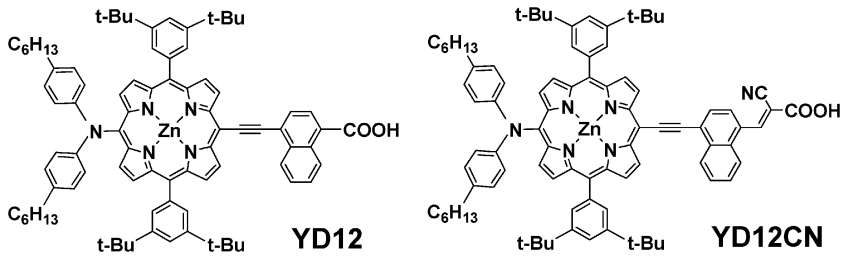

Chart 1 Molecular structures of YD12 and YD12CN.

2. Results and discussion

The details of synthesis and electrochemical results (Fig. S1 and S2, Table S1, ESI†) of YD12CN are given in ESI.† Fig. 1 shows the absorption spectra of YD12 and YD12CN in THF solutions (solid curves) and on TiO_2 films (dashed curves). In comparison with the YD12 spectrum in solution, introduction of the cyanoacrylic group in YD12CN leads to a red shift of both Soret and Q bands, but with much smaller absorption coefficients. When both molecules were sensitized on TiO_2 films, the spectra became significantly broadened relative to those in solutions with an absorption dip in the 550–600 nm spectral region. These two porphyrin dyes were fabricated into DSSC devices for photovoltaic and electron-transfer kinetic characterizations.

2.1 Photovoltaic properties

The effects of TBP concentrations on photovoltaic performance of the devices made of YD12 and YD12CN were studied at eight concentrations within a broad range (0.0–1.2 M); the *J–V* curves and the corresponding photovoltaic parameters are shown in Fig. S3 and S4 (ESI†), respectively. The results indicate that the best performance of the YD12 device appeared at the TBP concentration of 0.5 M, whereas the effect of TBP concentration for the YD12CN device was not evident in the range of 0–0.5 M. Because high TBP concentrations (>0.5 M) led to a significant decrease in photocurrent densities but limited improvement in photovoltages, we thus focus our investigations only on two conditions: the absence (0.0 M) and presence (0.5 M) of the TBP additive. Fig. 2a and b show the *J–V* curves and the corresponding IPCE action spectra for the YD12 and YD12CN devices, respectively; the obtained photovoltaic parameters and the amounts of dye-loading (DL) are summarized in Table 1. In those figures, the solid curves represent the devices with the TBP additive (0.5 M) in the electrolyte whereas the dashed curves represent those in the absence of TBP.

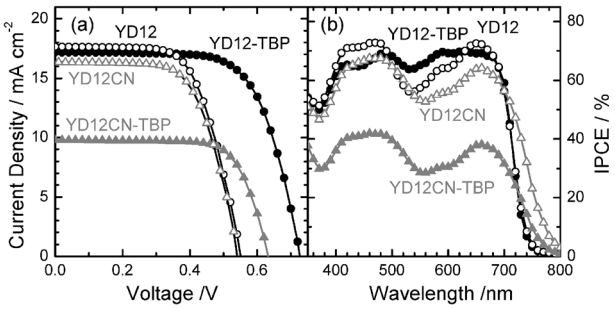

Fig. 2 Optimized photovoltaic properties: (a) current–voltage characteristics and (b) the corresponding IPCE action spectra of devices made of YD12 (black circles) and YD12CN (gray triangles) with (filled symbols) and without (open symbols) addition of TBP.

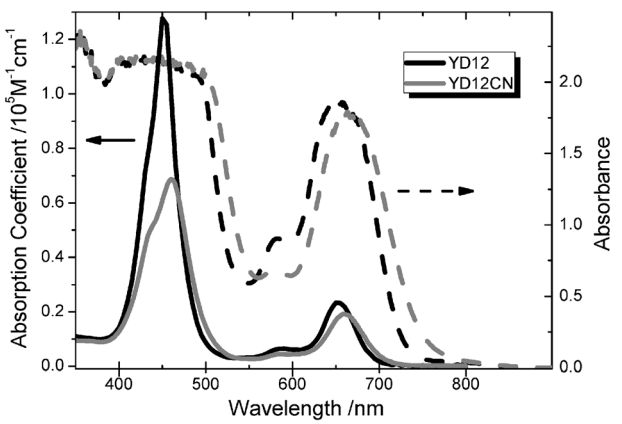

Fig. 1 Absorption spectra of YD12 (black) and YD12CN (gray) in THF (solid curves, absorption coefficients shown on the left axis) and on TiO_2 films (dashed curves, absorbance shown on the right axis).

TBP is a well-known electrolyte additive to modify the surface of TiO_2 for increasing the open-circuit voltage (V_{OC}).[1b,10] In the absence of TBP, both YD12 and YD12CN devices show similar photovoltaic performance with the short-circuit current density (J_{SC}) of the former being slightly larger than the latter. In the presence of TBP, the V_{OC} of YD12 increased dramatically from 550 to 729 mV while that of YD12CN only increased from 544 to 636 mV. On the other hand, the decrease of J_{SC} of the YD12 device was very small (from 17.65 down to 17.19 mA cm^{-2}) while the decrease of J_{SC} of the YD12CN device was quite substantial (from 16.45 down to 9.78 mA cm^{-2}). Therefore, addition of TBP in the YD12 device did help in boosting up

Table 1 Photovoltaic parameters and amounts of dye-loading of DSSCs fabricated with YD12 and YD12CN adsorbed on the TiO_2 films of thickness (12 + 5) μm under simulated AM-1.5G illumination (power 100 mW cm^{-2}) and an active area of 0.16 cm^2

Dye	DL/nmol cm^{-2}	J_{SC}/mA cm^{-2}	V_{OC}/mV	FF	η/%
YD12	255	17.65	550	0.643	6.2
YD12-TBP		17.19	729	0.677	8.5
YD12CN	213	16.45	544	0.642	5.8
YD12CN-TBP		9.78	636	0.716	4.5

the cell performance from η = 6.2% to 8.5%, but in the case of YD12CN it reduced from η = 5.8% to 4.5%. The IPCE spectra shown in Fig. 2b indicate a red-shifted feature for the YD12CN device, consistent with the absorption spectra shown in Fig. 1. The difference in the amounts of dye-loading might reasonably explain the discrepancy in J_{SC} in the absence of TBP. However, the significant reduction in IPCE and J_{SC} of the YD12CN device in the presence of TBP indicates that either poor electron injection or charge-collection yield is involved. To understand the electron transfer kinetics affecting the photovoltaic performance mentioned above, time-resolved investigations were performed.

2.2 Electron transport and kinetics of charge recombination of devices

The kinetics of electron transport of the devices made of YD12 and YD12CN with and without addition of TBP were deduced from the transient photoelectric (ΔJ_{SC} and ΔV_{OC} *vs.* time) and charge-extraction (CE) measurements[11] based on eight white-light (WL) intensities as bias irradiation sources (power densities in a range of 27–115 mW cm^{-2}); the resulting photovoltage decays are shown in Fig. S5–S8 (ESI†). Decay curves of the four devices for ΔV_{OC} *vs.* time were fitted according to a single exponential decay function to determine time coefficients for charge recombination (τ_R), transients of the four devices for ΔJ_{SC} *vs.* time were integrated to give the induced charge (ΔQ) due to the probe light irradiation, and the potential difference (ΔV) due to the probe irradiation was determined by the peak amplitude of the transient of ΔV_{OC} *vs.* time; the corresponding parameters are provided in Tables S2–S5 (ESI†).

As chemical capacitance ($C_\mu = \Delta Q/\Delta V$) is proportional to the density of states (DOS) of TiO_2 at the Fermi level,[11] the plots shown in Fig. 3 provide direct information on the shift of the conduction band edge of TiO_2 upon uptake of two different dyes in the presence or absence of TBP. In the absence of TBP, the potential of TiO_2 of the YD12CN device is located above ~50 mV compared to that of the YD12 device. In the presence of TBP, the TiO_2 potential of YD12CN shifts upward by only ~80 mV whereas that of YD12 shifts upward by as much as ~200 mV, compared to their non-TBP counterparts. The observed potential shifts are consistent with the enhancement in V_{OC} upon TBP addition:[10] the increment in V_{OC} is 92 and 179 mV for YD12CN and YD12, respectively (Table 1).

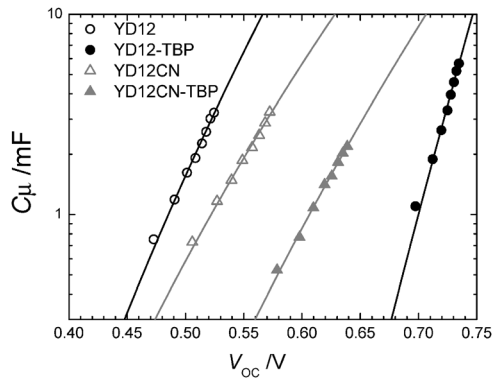

Fig. 3 Plots of chemical capacitance (C_μ) *vs.* V_{OC} for DSSC devices without TBP (black open circles and gray open triangles for YD12 and YD12CN, respectively) and for those with TBP (black filled circles and gray filled triangles for YD12 and YD12CN, respectively) under eight white bias light irradiations. The active area of the devices is 0.16 cm^2.

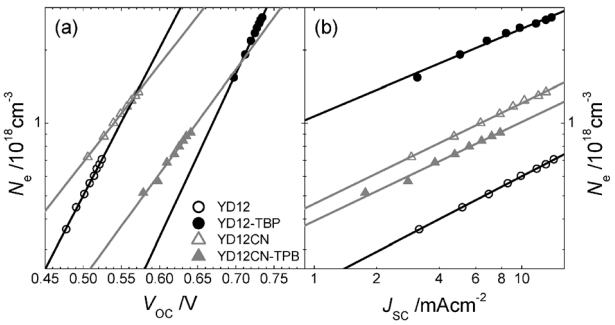

Fig. 4 (a) Semi-logarithmic plots of electron density (N_e) *vs.* V_{OC} and (b) logarithmic plots of N_e *vs.* J_{SC} for DSSC devices without TBP (black open circles and gray open triangles for YD12 and YD12CN, respectively) and for those with TBP (black filled circles and gray filled triangles for YD12 and YD12CN, respectively) under eight white bias light irradiations.

The charge densities (N_e) of the devices under certain bias light irradiation and under open-circuit conditions were determined *via* CE measurements when the circuit of the system was switched to the short-circuit condition. Fig. 4a and b show plots of log(N_e) *vs.* V_{OC} and log(N_e) *vs.* log(J_{SC}), respectively. Because N_e represents the number of extracted charges under bias light irradiation, the deviation of the N_e *vs.* V_{OC} plots from a standard plot provides information on potential band-edge movements, whereas the deviation of the N_e *vs.* J_{SC} plots from a standard plot gives information on the extent of charge recombination.[12] According to the V_{OC} *vs.* N_e plots shown in Fig. 4a, we observed an almost equivalent potential up-shift (~120 mV) upon adding TBP in both YD2 and YD2CN devices. The potential variation is different from what we observed in Fig. 3 because N_e counts all the charges below the Fermi level whereas C_μ represents the DOS only at the Fermi level. This observation is consistent with that of a Z907 system containing various guanidine coadsorbents, for which the plots of C_μ *vs.* V_{OC} reflect the true movement of the conduction band edge whereas interpretation of the N_e *vs.* V_{OC} variations requires further information on the effect of charge recombination.[13]

Plots of N_e *vs.* J_{SC} shown in Fig. 4b predict the effects of charge recombination for the two systems – addition of TBP significantly retarded charge recombination hence the charge density increased for YD12, but it had a negative effect of enhancing charge recombination hence the charge density decreased for YD12CN. The same phenomena for the plots of τ_R *vs.* N_e are shown in Fig. 5, which shows that TBP in the YD12 device has succeeded in modifying the surface of TiO_2 for significant retardation of τ_R (shown as circle symbols). However, in the case of YD12CN we observed an opposite effect upon addition of TBP (shown as triangle symbols), for which charge recombination became a more severe problem in the presence of TBP. According to the results shown in Fig. 4a, the TiO_2 potentials were up-shifted by ~120 mV upon addition of

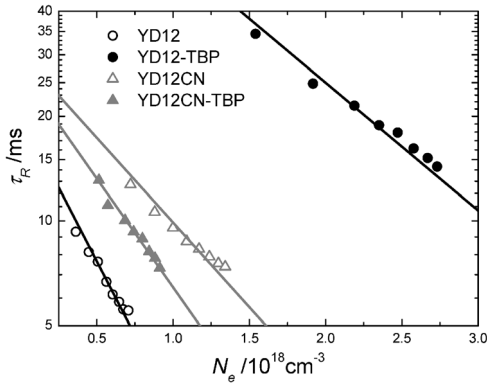

Fig. 5 Semi-logarithmic plots of charge recombination time coefficient (τ_R) *vs.* electron density (N_e) for DSSC devices without TBP (black open circles and gray open triangles for YD12 and YD12CN, respectively) and for those with TBP (black filled circles and gray filled triangles for YD12 and YD12CN, respectively) under eight white bias light irradiations.

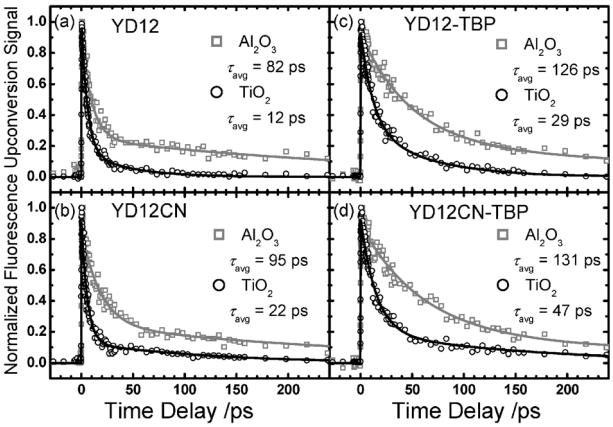

Fig. 6 Femtosecond fluorescence decays of thin-film samples sensitized with (a) YD12 and (b) YD12CN in the absence of TBP and (c) YD12 and (d) YD12CN in the presence of TBP. The black circles and gray squares represent the data obtained from the dyes sensitized on TiO_2 and Al_2O_3 films, respectively, and the solid traces represent the theoretical fits according to a bi-exponential decay function. The excitation was performed at 435 nm and the emissions were optically gated at 710 nm and 730 nm for YD12 and YD12CN, respectively.

TBP in both devices; the retardation and acceleration of charge recombination for YD12-TBP and YD12CN-TBP, respectively, reasonably account for the increase of V_{OC} by 179 and 92 mV for the former and the latter, respectively. Such an observation indicates that the YD12CN-TBP device involves poor charge collection yields accounting for the observed low IPCE values leading to the poor J_{SC} as indicated in Fig. 2. We propose that, in the presence of TBP, the floppy YD12CN might be tilted further on the surface of TiO_2 for the charge recombination to occur more rapidly.[14]

2.3 Interfacial electron transfer dynamics of sensitized films

Femtosecond excitation of the thin-film samples immersed in acetonitrile solvent was performed at 435 nm using a fluorescence up-conversion system described elsewhere.[8a,9,15] The emissions at the intensity maximum (710 nm for YD12 and 730 nm for YD12CN) were optically gated with the fundamental pulse (870 nm) to yield the emission decays. Fig. 6a–d show the decays of the YD12- and YD12CN-sensitized TiO_2 films without and with TBP; those of the sensitized Al_2O_3 films under similar experimental conditions are also shown for comparison. The temporal profiles of all samples exhibit a bi-exponential decay feature and the corresponding time coefficients were obtained upon analyzing the data with a parallel kinetic model (Fig. S9 and S10, ESI†). To resolve the kinetics resulting from energy transfer and electron injection, we averaged the time coefficients according to the amplitude-averaged decay time model,[8a] the corresponding rate coefficients were determined according to $k_{TiO_2} = \tau_{TiO_2}^{-1}$ and $k_{Al_2O_3} = \tau_{Al_2O_3}^{-1}$; the average time coefficients of the TiO_2 and Al_2O_3 films are summarized in Tables S6 and S7 (ESI†).

The fluorescence decays of the porphyrin-sensitized Al_2O_3 films reflect only the intermolecular energy transfer because of aggregation of the dye on the Al_2O_3 surface, but the decays of the porphyrin-sensitized TiO_2 films not only contain the aggregate-induced energy transfer but also reflect the rapid electron injection from the excited state of the dye into the conduction band of TiO_2. If we assume that the extent of dye aggregation on both TiO_2 and Al_2O_3 films is similar,[8a,9] based on the same amount of dye molecules adsorbed on the films (Fig. S11, ESI†), the electron injection yields of the YD12 and YD12CN sensitized TiO_2 films in the absence of TBP were evaluated to be Φ_{inj} = 0.85 and 0.77, respectively. In the presence of TBP, the emission decays slow down for all cases and the evaluated Φ_{inj} values of the YD12 and YD12CN films are 0.77 and 0.63, respectively. Note that the intrinsic electron injection yield of YD12CN (no TBP addition) is smaller than that of YD12 due to a substantially slower rate of electron injection of the former than the latter. As shown for the results of Al_2O_3 films, addition of TBP reduces the rate of intermolecular energy transfer ($k_{avg}/10^{10}$ s^{-1}) more significantly for YD12 than for YD12CN (0.8/1.2 *vs.* 0.8/1.0), but the extent of reduction in the electron injection rate ($k_{inj}/10^{10}$ s^{-1}) is similar for both dyes (2.7/6.9 *vs.* 1.3/3.6). The role played by TBP in reducing Φ_{inj} can thus be understood as being due to retardation of the electron injection rates and the intermolecular energy transfer rates to a different extent; the former reduction is due to the up-shifts of the TiO_2 potentials and the latter reduction arises from the protective effect of TBP surrounding the porphyrin sensitizers.

3. Conclusion

We have examined the effects of the TBP additive on device performance for two push–pull porphyrins (YD12 and YD12CN) based on time-resolved investigations of thin-film samples using femtosecond fluorescence up-conversion spectroscopy, charge extraction and transient photoelectric measurements of the corresponding devices. We found that, without addition of TBP, the device performance of the two dyes is similar, but in the presence of TBP (0.5 M) the power conversion efficiencies of the YD12 device increase from 6.2% to 8.5% whereas those of the YD12CN device decrease from 5.8% to 4.5%. For YD12,

the great enhancement in V_{OC} from 550 (no TBP) to 729 mV (with TBP) is mainly due to a large upward shift of the TiO_2 potential and the significant retardation of charge recombination and the small degradation of J_{SC} upon TPB addition are due to reduction of electron-injection yields for the up-shifted TiO_2 potential. For YD12CN, the small enhancement of V_{OC} from 544 (no TBP) to 636 mV (with TBP) is also due to an upward shift of the TiO_2 potential to a lesser extent, but the dramatic reduction of J_{SC} from 16.45 (no TBP) to 9.78 mA cm^{-2} (with TBP) arises from two major factors: (1) the acceleration of charge recombination leading to poor charge-collection yields and (2) the retardation of electron injection leading to poor electron-injection yields. We also found that the intermolecular energy transfer was inhibited in the presence of TBP, and the extent of inhibition was found to be much inferior for YD12CN than for YD12, giving much smaller electron-injection yields for the former than for the latter.

Acknowledgements

National Science Council of Taiwan and Ministry of Education of Taiwan, under the ATU program, provided support for this project.

References and notes

1 (*a*) M. Grätzel, *Acc. Chem. Res.*, 2009, **42**, 1788–1798; (*b*) A. Hagfeldt, G. Boschloo, L. Sun, L. Kloo and H. Pettersson, *Chem. Rev.*, 2010, **110**, 6595–6663.

2 (*a*) M. K. Nazeeruddin, A. Kay, I. Rodicio, R. Humphry-Baker, E. Müller, P. Liska, N. Vlachopoulos and M. Grätzel, *J. Am. Chem. Soc.*, 1993, **115**, 6382–6390; (*b*) N. Robertson, *Angew. Chem., Int. Ed.*, 2006, **45**, 2338–2345.

3 (*a*) H. Imahori, T. Umeyama and S. Ito, *Acc. Chem. Res.*, 2009, **42**, 1809–1818; (*b*) M. V. Martínez-Díaz, G. de la Torre and T. Torres, *Chem. Commun.*, 2010, **46**, 7090–7108; (*c*) L.-L. Li and E. W.-G. Diau, *Chem. Soc. Rev.*, 2013, **42**, 291–304.

4 (*a*) G. Zhang, H. Bala, Y. Cheng, D. Shi, X. Lv, Q. Yu and P. Wang, *Chem. Commun.*, 2009, 2198–2200; (*b*) Z. Ning and H. Tian, *Chem. Commun.*, 2009, 5483–5495; (*c*) Y. Ooyama and Y. Harima, *Eur. J. Org. Chem.*, 2009, 2903–2934; (*d*) Y. Wu, X. Zhang, W. Li, Z.-S. Wang, H. Tian and W. Zhu, *Adv. Energy Mater.*, 2012, **2**, 149–156.

5 Q. Yu, Y. Wang, Z. Yi, N. Zu, J. Zhang, M. Zhang and P. Wang, *ACS Nano*, 2010, **4**, 6032–6038.

6 T. Bessho, S. M. Zakeeruddin, C.-Y. Yeh, E. W.-G. Diau and M. Grätzel, *Angew. Chem., Int. Ed.*, 2010, **49**, 6646–6649.

7 A. Yella, H.-W. Lee, H. N. Tsao, C. Yi, A. K. Chandiran, M. K. Nazeeruddin, E. W.-G. Diau, C.-Y. Yeh, S. M. Zakeeruddin and M. Grätzel, *Science*, 2011, **334**, 629–634.

8 (*a*) H.-P. Lu, C.-Y. Tsai, W.-N. Yen, C.-P. Hsieh, C.-W. Lee, C.-Y. Yeh and E. W.-G. Diau, *J. Phys. Chem. C*, 2009, **113**, 20990–20997; (*b*) C.-P. Hsieh, H.-P. Lu, C.-L. Chiu, C.-W. Lee, S.-H. Chuang, C.-L. Mai, W.-N. Yen, S.-J. Hsu, E. W.-G. Diau and C.-Y. Yeh, *J. Mater. Chem.*, 2010, **20**, 1127–1134.

9 H.-P. Lu, C.-L. Mai, C.-Y. Tsia, S.-J. Hsu, C.-P. Hsieh, C.-L. Chiu, C.-Y. Yeh and Eric W.-G. Diau, *Phys. Chem. Chem. Phys.*, 2009, **11**, 10270–10274.

10 (*a*) G. Boschloo, L. Haggman and A. Hagfeldt, *J. Phys. Chem. B*, 2006, **110**, 13144–13150; (*b*) R. Katoh, M. Kasuya, S. Kodate, A. Furube, N. Fuke and N. Koide, *J. Phys. Chem. C*, 2009, **113**, 20738–20744; (*c*) Z. Ning, Y. Fu and H. Tian, *Energy Environ. Sci.*, 2010, **3**, 1170–1181.

11 (*a*) L. Luo, C.-J. Lin, C.-S. Hung, C.-F. Lo, C.-Y. Lin and E. W.-G. Diau, *Phys. Chem. Chem. Phys.*, 2010, **12**, 12973–12977; (*b*) L.-L. Li, Y.-C. Chang, H.-P. Wu and E. W.-G. Diau, *Int. Rev. Phys. Chem.*, 2012, **31**, 420–467.

12 N. Kopidakis, N. R. Neale and A. J. Frank, *J. Phys. Chem. B*, 2006, **110**, 12485–12489.

13 Z. Zhang, N. Evans, S. M. Zakeeruddin, R. Humphry-Baker and M. Grätzel, *J. Phys. Chem. C*, 2007, **111**, 398–403.

14 (*a*) H. Imahori, S. Kang, H. Hayashi, M. Haruta, H. Kurata, S. Isoda, S. E. Canton, Y. Infahsaeng, A. Kathiravan, T. Pascher, P. Chábera, A. P. Yartsev and V. Sundström, *J. Phys. Chem. A*, 2011, **115**, 3679–3690; (*b*) S. Mathew, H. Iijima, Y. Toude, T. Umeyama, Y. Matano, S. Ito, N. V. Tkacheko, H. Lemmetyinen and H. Imahori, *J. Phys. Chem. C*, 2011, **115**, 14415–14424.

15 L. Luo, C.-J. Lin, C.-Y. Tsai, H.-P. Wu, L.-L. Li, C.-F. Lo, C.-Y. Lin and E. W.-G. Diau, *Phys. Chem. Chem. Phys.*, 2010, **12**, 1064–1071.